Low Temperature Physics/Fizika Nizkikh Temperatur, 2016, v. 42, No. 7, pp. 743–747

Optical absorption and luminescence studies of fast neutron-irradiated complex oxides for jewellery applications

N. Mironova-Ulmane, V. Skvortsova, and A.I. Popov

Institute of Solid State Physics, University of Latvia, 8 Kengaraga Str., Riga LV-1063, Latvia
E-mail: nina@cfi.lu.lv

Received May 12, 2016, published online May 25, 2016

We studied the optical absorption and luminescence of agate (SiO_2), topaz ($Al_2[SiO_4](F,OH)_2$), beryl ($Be_3Al_2Si_6O_{18}$), and prehnite ($Ca_2Al(AlSi_3O_{10})(OH)_2$) doped with different concentrations of transition metal ions and exposed to fast neutron irradiation. The exchange interaction between the impurity ions and the defects arising under neutron irradiation causes additional absorption as well as bands' broadening in the crystals. These experimental results allow us to suggest the method for obtaining new radiation-defect induced jewellery colors of minerals due to neutron irradiation.

PACS: 61.80.Hg Neutron radiation effects;
61.80.–x Physical radiation effects, radiation damage;
78.60.–b Other luminescence and radiative recombination.

Keywords: absorption, luminescence, neutron irradiation.

1. Introduction

Nuclear reactors are widely used in industry to produce materials with new properties. The development of modern radiation technologies for modifying the properties of materials and products for the electronic, medical, pharmaceutical and food industries implies further research of particles and radiation interaction with these materials. Natural and synthetic minerals — e.g. topaz, beryl, etc. — are used not only as gemstones but also used in practice. For example, topaz crystals are suitable material for dosimetric applications [1,2]. In turn, beryl crystals doped with transition metal ions find applications as laser materials [3]. Most gemstone crystals have intrinsic colors, that are caused by the optical absorption and presence of color centers due to transition metal- and rare-earth ions or defects in crystalline lattice [4]. Point defects and their complexes in the crystalline structure affect many physical properties and allow use of these crystals in practice. Currently, artificial precious stones colored by radiation are widely distributed. Many gems may acquire intense colors by exposing them to various forms of radiation, such as fast electrons, gamma rays, or neutrons. Optical absorption spectra have been reported for beryl, topaz, agate and prehnite crystals [5–8]; however, the origin of these colors in minerals is not well understood. On the other hand, the nature of radiation defects in more simple oxides is understood much better [9–27].

The paper presents the results of neutron irradiation on the optical properties of topaz $Al_2[SiO_4](F, OH)_2$, beryl $Be_3Al_2Si_6O_{18}$ (natural and synthetic), prehnite $Ca_2Al(AlSi_3O_{10})(OH)_2$ and agate SiO_2 crystals.

2. Experimental details

The standard technique for measuring absorption spectra is based on a "Specord M-40" double-beam spectrometer operating in the 200–900 nm region and "Specord 210" (Analytikjena) double-beam spectrophotometer operating in the spectral region of 190–1100 nm.

A conventional experimental setup was used for measurements of photoluminescence (PL). In photoluminescence measurements at low temperatures a sample was placed into refregerator "Janis", providing temperature range from 8 to 300 K.

In surface investigations we used computer-aided image automatic analyzer "MORPHOQUANT" with a video camera.

The neutron irradiations were performed at the Latvian 5 MW water-water research reactor. The fluence of fast neutrons with energy 0.1 MeV was in the range 10^{14}–$5{\cdot}10^{18}$ cm^{-2}. A cadmium filter was used for absorption of thermal neutrons.

3. Results and discussion

A natural topaz stone with the structure of aluminum silicate fluoride hydroxide $Al_2[SiO_4](F, OH)_2$ is usually colorless and thus have no value. Figure 1 shows the absorption spectra of topaz single crystals. The absorption spectra of colorless topaz before fast neutron irradiation contain an absorption band at 230 nm (Fig. 1, curve *1*). The intensity of this absorption band after irradiation increases with appearance of new bands with maxima at 305, 430 and 620 nm (Fig. 1, curve *2*, *3*); thus crystals obtain a blue color. In the natural blue topaz the intensive band at 230 nm and less intensive bands at 430 and 620 nm were also identified (Fig. 1, curve *4*). Two lines around 230 and 305 nm belong to a single defect such as silanone (=Si=O) as it was suggested in [28] based on similar lines observed in spodumene. A blue color is related to a broad absorption band in the red part of the spectrum generated by the so-called *R*-centers (two *F*-vacancies with two trapped electrons) [29]. It was previously concluded that the optical absorption band centered at 620 nm is closely correlated with the O^- center interacting with two Al ions in the topaz structure [30]. This O^- center is produced by irradiation in the hydroxyl sites which substitutes for fluorine in the topaz structure [31].

As suggested by Priest *et al*. [32], the defects in neutron-irradiated topaz reveal a doubly-occupied dangling silicon bond. The calculations [33] using an $AlCrFH_7O_{11}Si$ model molecule have shown that the theoretical spectrum is indeed in a very good agreement with the experimental one. The excitation spectra of Cr^{3+} impurity ions [34] in a topaz crystal show the same lines. Considering the above mentioned results and our own results [35,36], we assume that the absorption band at 620 nm includes not only the above mentioned bands, but also those associated with the presence of impurities of Cr^{3+}, Fe^{2+} and Mn^{2+} ions. The band 430 nm is due to Cr^{3+} impurity ions.

Beryl is the most alluring and popular mineral. It could reveal diverse colours met in several important gemstone depositions. The color of beryl $Be_3Al_2Si_6O_{18}$ is usually determined by the Fe^{2+} and Fe^{3+} content. The former produces pale blue color, while Fe^{3+} produces golden-yellow color; while when both Fe^{2+} and Fe^{3+} are present, the color is dark blue. A green color in the iron-containing beryl usually results from a mixture of blue and yellow components. Green color can also arise from Cr^{3+} as was found in various emeralds. The silicon-oxygen motif of beryl $Be_3Al_2Si_6O_{18}$ crystal structure (space group *P*6/*mcc*) represents isolated six-member rings $[Si_6O_{18}]$ lying in the (0001) plane. These rings are joined into a single framework structure via the Al octahedral and Be tetrahedral at levels of ¾ and ¼ along the *c*-axis of the hexagonal unit cell. The sixfold axis passes through the centers of $[Si_6O_{18}]$ rings and is the geometrical axis of channels (2.5–5.0 Å in diameter), which can be occupied by large-sized low-charged cations and/or water molecules. The presence of these components in variable amounts and different framework positions — primarily, octahedral positions (substitution of Fe, Cr, Sc, V, Mn, Mg atoms for Al atoms) — is responsible for the fact that natural samples often differ significantly in composition from $Be_3Al_2Si_6O_{18}$. Though beryl is naturally transparent, inclusions and impurities may make it opaque.

The photoluminescence spectra of flux beryl at different excitation wavelength and at 8 K are given in Fig. 2. A wide band at 740 nm is related to Fe^{2+} ions, while narrow lines in region from 680 to 720 nm belong to single Cr^{3+} (*R*-lines) ions and Cr^{3+}-pairs (*N*-lines). The intensity of the photoluminescence band at 525 nm increases as temperature decreases. Synthetic beryl crystals containing chromium ions impurity have a more saturated color than natural crystals.

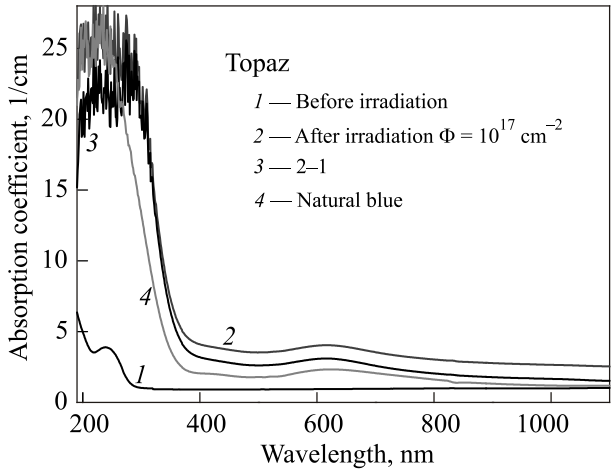

Fig. 1. Topaz absorption spectra: before irradiation (*1*), after fast neutron irradiation 10^{17} cm^2 (*2*), additional absorption spectra (2–1) (*3*), Absorption spectrum of natural blue topaz from Ukraine (*4*).

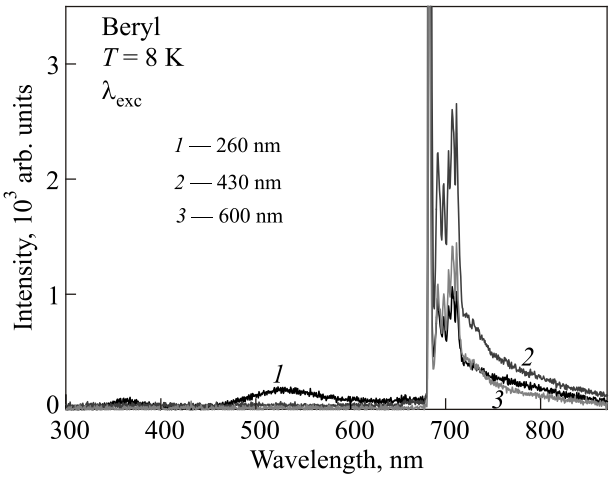

Fig. 2. Photoluminescence spectra of Beryl flux crystal at different excitation wavelengths, measured at temperature $T = 8$ K.

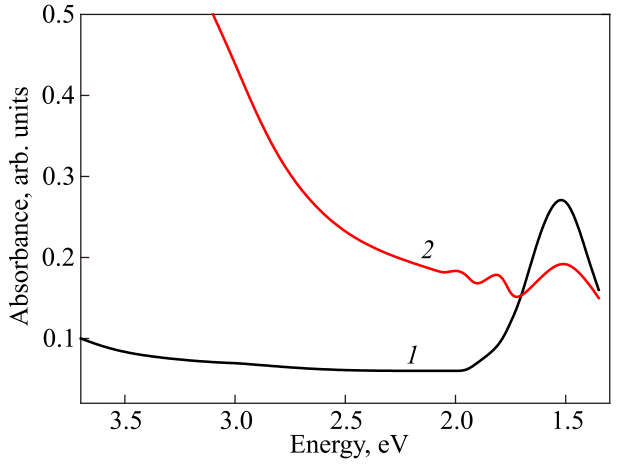

Fig. 3. Absorption spectra of pale blue beryl (*1*) before and (*2*) after neutron irradiation.

Beryl crystals studied in the present work before irradiation had only the absorption band associated with Fe ions in octahedral environment (Fig. 3, curve *2*). The wide absorption band with a peak in the near-infrared range at 820 nm is observed in all spectra. This band is generally ascribed to the internal electron transition of $^5T_2$ (^5D) $\rightarrow$ ^5E (^5D) in Fe^{2+} ions, localized in octahedral aluminum sites of beryl [37,38]. These crystals contain a small amount of chromium ions. There were no absorption bands, prior to irradiation, associated with the electronic transitions $^4A_{2g}$ (F) $\rightarrow$ $^4T_{2g}$ (F) (630 nm) and $^4A_{2g}$ (F) $\rightarrow$ $^4T_{1g}$ (F) (431 nm). Under the impact of fast neutron fluence of 10^{13}–10^{17} cm^{-2}, the intensity of 813 nm band reduces and the absorption edge shifts due to appearance of intense absorption band in the UV region. Besides, after irradiation an additional band arises with maximum at 690 nm, connected with zero phonon transition $^4A_{2g}$ (F) $\rightarrow$ ^2E_g (G) in Cr^{3+} ion. Dependence of the absorption band intensity at 813 nm (curve *1*) and 694 nm (curve *2*) on the fast neutron fluence in a pale blue beryl is shown on Fig. 4. As earlier reported [39–43], an irradiation produces NO_3^0 and CO_3^- type radicals, which seem to be related to blue colors in a beryl. We suppose that the band with the maximum at 690 nm belongs to a complex center consisting of Cr^{3+} ions and radiation defects. Presence of Fe^{2+} ions contributes to the persistence of the complex defect [44].

Agate is a form of chalcedony which is a variety of quartz. It is composed primarily of microscopically crystallized silica (SiO_2) and often occurs as a cavity filling in lavas [45,46]. Agate is formed in layers and usually follows the shape of the cavity. The most common use for agate is as an ornamental stone. It is used for jewellery, vases, book ends, sculptures, tabletops and tiles. Natural colors are brown, black, tan and white. Since agate slices come from geodes and nodules, the shapes of the slice reflects the most common geode ones. The most common shapes are round and oval. Figure 5 shows the agate light penetration curves for natural and ennobled agate. Neutron irradiation is used for a production of a more contrast color of agate.

Prehnite is a rock-forming mineral. It occurs in association with calcite, quartz, zoisite, granites, rocks and minerals. Prehnite replaces the primary minerals and also appears in veins and druses [47]. This is a semi-transparent stone, which, when of a deep oil-green colour, may have a limited use in jewelry. The usual transition metal ion that occurs in many mineral samples is iron. This stone is transparent, and shows a pale-apple green or pale-yellow or greyish white colors. Prehnite $Ca_2Al(AlSi_3O_{10})(OH)_2$ has the orthorhombic phase (space group *P2cm*) with two formula units in unit cell [48]. The unit cell parameters are a = 4.646 Å, b = 5.49 Å and c = 18.52 Å [49].

The absorption spectra of prehnite irradiated by fast neutron with fluence 10^{16} cm^{-2} are similar to those of γ-irradiated crystal [49]. The bands at 455 nm and 518 nm arise, as fluence increases (Fig. 6). If the iron concentration is high enough, the 455 nm and 518 nm bands start to overlap with the wide intensive band at 667–555 nm, connected with the exchange interaction of $Fe^{2+}_{oct} \rightarrow Fe^{3+}_{tetr}$. The 518 nm band belongs to V_{OH}- centers, the 455 nm band — to V^--centre

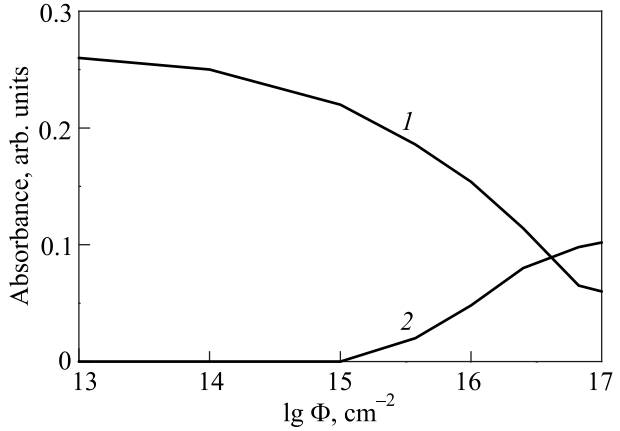

Fig. 4. Pale blue beryl absorption band 813 nm (*1*) and 694 nm (*2*) intensities as functions of fast neutron fluence.

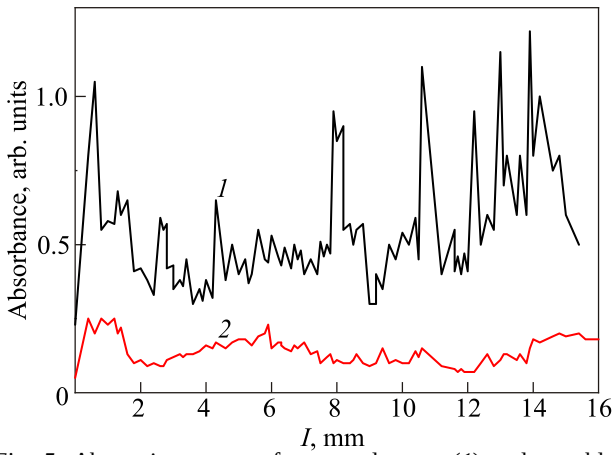

Fig. 5. Absorption spectra for natural agate (*1*) and ennobled agate (*2*).

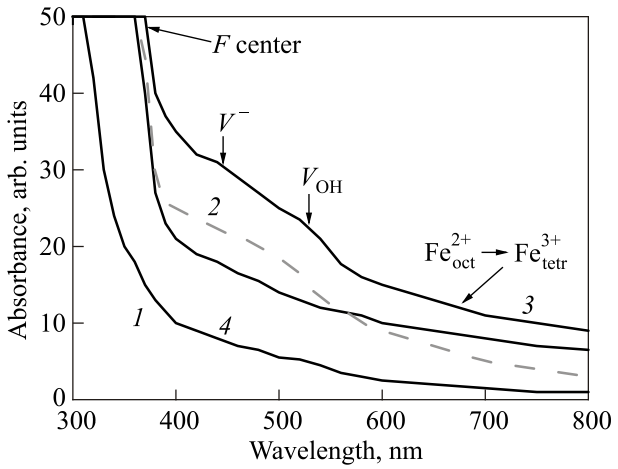

Fig. 6. Prehnite absorption spectra: before irradiation (*1*), after fast neutron irradiation $1.2\cdot10^{16}$ cm^{-2} (*2*), after neutron irradiation $2.5\cdot10^{16}$ cm^{-2} (*3*), annealed at 403 K during 10 min (*4*).

and the 357 nm band — to the *F*-centre. These experimental results allow us to suggest make a method for obtaining new jewellery colors other than green, which is induced only due to radiation defects [50].

4. Conclusions

Based on the results of our investigation of the optical absorption of topaz, beryl (natural and synthetic), prehnite and agate crystals before and after neutron irradiation the following conclusions could be drawn.

Defects produced in the minerals under fast neutron irradiation with fluences up to $5\cdot10^{18}$ cm^{-2} ($E > 0.1$ MeV) are responsible for the colors observed in the irradiated samples.

An irradiation leads to the formation of two types of complex centers: Me^{2+}–F^+ (or *F*) center and complex centers consisting of a cation vacancy and an impurity (iron, manganese) ion.

The exchange interaction in Me Me^{2+}–F^+ (or *F*) center pairs results in an enhanced intensity of the spin-forbidden transitions in single crystals.

A deep insight into the origin of mineral colors would allow us to predict the quality of colors produced by artificial coloration.

The experimental results presented here make it possible to develop the method for producing new jewellery colors that would be induced only by radiation defects.

Acknowledgments

This work was supported by Latvian Science Council Grant No 402/2012.

1. C.M.S. de Magalhaes, Z.S. Macedo, M.E.G. Valerio, A.C. Hernandes, and D.N. Souza, *Nucl. Instr. Meth. B* **218**, 277 (2004).
2. D.N. Souza, M.E.G. Valerio, J.F. de Lima, and L.V.E. Caldas, *Nucl. Instr. Meth. Phys. Res. B* **166–167**, 209 (2000).
3. Fuxi Gan, *Laser Materials*, World Scientific (1995).
4. B. Henderson, *Contemp. Phys.* **19**, 225 (1978).
5. L.O. Anderson, *J. Gemmology* **32**, 145 (2011).
6. S. Isotoni, A.R. Blak, and S. Watanabe, *Physica B* **405**, 1501 (2010).
7. T.A. Detrie, N.L. Ross, R.J. Angel, and M.D. Welch, *Mineral. Mag.* **72**, 1163 (2008).
8. V.Yu. Ivanov, V.A. Pustovarov, E.S. Shlygin, A.V. Korotaev, and A.V. Kruzhalov, *Phys. Solid State* **47**, 466 (2005).
9. E.A. Kotomin, A.I. Popov, and A. Stashans, *J. Phys. Condens. Matter* **6**, L569 (1994).
10. E.A. Kotomin and A.I. Popov, *Nucl. Instr. Meth. B* **141**, 1 (1998).
11. M.A. Monge, R. González, J.E. Muñoz, Santiuste, R. Pareja, Y. Chen, E.A. Kotomin, and A.I. Popov, *Phys. Rev. B* **60**, 3787 (1999).
12. S.B. Ubizskii, A.O. Matkovskii, N. Mironova-Ulmane, V. Skvortsova, A. Suchocki, Y.A. Zhydachevskii, and P. Potera, *Phys. Status Solidi A* **177**, 349 (2000).
13. M.A. Monge, R. González, J.E. Muñoz Santiuste, R. Pareja, Y. Chen, E.A. Kotomin, and A.I. Popov, *Nucl. Instr. Meth. B* **166**, 220 (2000).
14. S.B. Ubizskii, A.O. Matkovskii, N. Mironova-Ulmane, V. Skvortsova, A. Suchocki, Y.A. Zhydachevskii, and P. Potera, *Nucl. Instr. Meth. B* **166**, 40 (2000).
15. T. Kärner, S. Dolgov, N. Mironova-Ulmane, S. Nakonechnyi, and E. Vasil'chenko, *Radiat. Measur.* **33**, 625 (2001).
16. T. Kärner, S. Dolgov, A. Lushchik, N. Mironova-Ulmane, S. Nakonechnyi, and E. Vasil'chenko, *Rad. Eff. Defect. Solids* **155**, 171 (2001).
17. V.N. Kuzovkov, A.I. Popov, E.A. Kotomin, M.A. Monge, R. Gonzalez, and Y. Chen, *Phys. Rev. B* **64**, 064102 (2001).
18. V. Skvortsova, N. Mironova-Ulmane, and U. Ulmanis, *Nucl. Instr. Meth. B* **191**, 256 (2002).
19. S. Dolgov, T. Kärner, A. Lushchik, A. Maaroos, N. Mironova-Ulmane, and S. Nakonechnyi, *Radiation Protection Dosimetry* **100**, 127 (2002).
20. E.A. Kotomin and A.I. Popov, *Radiation Effects in Solids*: *NATO Science Ser.* (2007), vol. 235, p. 153.
21. P. Potera, S. Ubizskii, Y. Zhydachevskii, D. Sugak, Solskii, and T. Lukasiewicz, *Rad. Eff. Defect. Solids* **162**, 821 (2007).
22. V. Skvortsova, N. Mironova-Ulmane, and U. Ulmanis, *Nucl. Instr. Meth. A* **580**, 434 (2007).
23. A.I. Popov, E.A. Kotomin, and J. Maier, *Nucl. Instr. Meth. B* **268**, 3084 (2010).
24. A.I. Popov, L. Shirmane, V. Pankratov, A. Lushchik, A. Kotlov, V.E. Serga, L.D. Kulikova, G. Chikvaidze, and J. Zimmermann, *Nucl. Instr. Meth. B* **310**, 23 (2013).
25. E. Shablonin, A.I. Popov, A. Lushchik, A. Kotlov, and S. Dolgov, *Physica B* **477**, 133 (2015).

26. A. Lushchik, Ch. Lushchik, A.I. Popov, K. Schwartz, E. Shablonin, and E. Vasil'chenko, *Nucl. Instr. Meth. B* **374**, 90 (2016).
27. E.A. Kotomin, V.N. Kuzovkov, A.I. Popov, and R. Vila, *Nucl. Instr. Meth. B* **374**, 107 (2016).
28. W. Bonventi Jr., S. Isotani, and A.R.P. Albuquerque, *Adv. Condens. Matter Phys.* **2012**, ID 873804 (2012).
29. A.N. Platonov, M.N. Taran, and V.S. Balyatskii, *Nature of Color Gems*, Nedra, Moscow (1984).
30. A.S. Leal, K. Krambrock, L.G.M. Ribeiro, M.A.B.C. Menezes, P. Vermaercke, and L. Sneyers, *Nucl. Instr. Meth. A* **580**, 423 (2007).
31. D.N. Da Silva, K.J. Guedes, M.V.B. Pinheiro, J.-M. Spaeth, and K. Krambrock, *Phys. Chem. Mineral.* **32**, 436 (2005).
32. V. Priest, D.L. Cowan, D.G. Reichel, and F.K. Ross, *J. Appl. Phys.* **68**, 3035 (1990).
33. H. Goto, A. Niwa, D.C. Greenhidge, N. Kato, T. Ida, M. Mizuno, K. Endo, and T. Tada, *J. Surf. Anal.* **12**, 249 (2005).
34. A.N. Tarashchan, M.N. Taran, H. Rager, and W. Iwanuch, *Phys. Chem. Mineral*. **32**, 679 (2006).
35. V. Skvortsova, N. Mironova-Ulmane, and L. Trinkler, *IOP Conf. Series: Mater. Science Engin*. **80**, 012008 (2015).
36. V. Skvortsova, N. Mironova-Ulmane, L. Trinkler, and G. Chikvaidze, *IOP Conf. Series: Mater. Science Engin*. **49**, 012051 (2013).
37. M.N. Taran and G.R. Rossman, *Am. Mineral.* **86**, 973 (2001).
38. G. Spinolo, I. Fontana, and A. Galli, *Phys. Status. Solidi B* **244**, 4660 (2007).
39. A.S. Marfunin, *Spectroscopy, Luminescence and Radiation Centres in Mineral*, Springer, Berlin (1979).
40. K. Nassau, B.E. Prescott, and D.L. Wood, *Am. Mineral*. **61**, 100 (1976).
41. L.O. Anderson, *J. Gemmology* **16**, 313 (1979).
42. A. Edgar and E.R. Vance, *Phys. Chem. Mineral***. 1**, 163 (1977).
43. V. Skvortsova, N. Mironova-Ulmane, L. Trinkler, and V. Merkulov, *IOP Conf. Series: Mater. Science Engin*. **77**, 012034 (2015).
44. *Gems: Their Sources, Description and Identification*, M. O'Donoughue (ed.), Elsevier Amsterdam (2006).
45. H.W. Dennen, *Principles of Mineralogy*, Ronald Press, New-York (1960).
46. N.C.G. Reddy, S.M. Fayazyddin, R.R.S. Reddy, G.S. Reddy, S. Lakshmi, P.S. Rao, and B.J. Reddy, *Spectrochim. Acta A* **62**, 71 (2005).
47. W.Y. Zhao, X.W. Liu, O.Y. Wang, and Q.J. Zhang, *Central China Mineral. Mag*. **67**, 73 (2003).
48. T.B. Zunic, S. Scavnicar, and G. Molin, *Eur. J. Miner*. **2**, 731 (1990).
49. G.S. Nazarova, B.A. Ostaschenko, V.Ya. Mitrofanov, O.Yu. Shilova, and L.D. Zaripova, *J. Appl. Spectrosc.* **53**, 890 (1990). (Translated from *Zhurnal Prikladnoi Spektroskopii*, Vol. 53, No. 2, pp. 305–310, February (1990)).
50. G.S. Nazarova, B.A. Ostaschenko, N.A. Mironova, O.Yu. Shilova, and V.Ya. Mitrofanov, *Method of Determining the Quality of Prehnite Used in the Jewelry Industry*, USSR, patent no. 517536 (1987).